DMA−FTIR Creep−Recovery Study of a Poly(ester urethane) Elastomer with Molecular-Level Viscoelastic Modeling

Haochuan Wang,[†] Darla Graff Thompson,[‡] Jon R. Schoonover,[‡] Steven R. Aubuchon,[§] and Richard A. Palmer*[,†]

Department of Chemistry, Duke University, Durham, North Carolina 27708; Materials Science and Technology Division, MS E549, Los Alamos National Laboratory, Los Alamos, New Mexico 87545; and TA Instruments, Inc., 109 Lukens Drive, New Castle, Delaware 19720

Received October 16, 2000; Revised Manuscript Received June 14, 2001

ABSTRACT: The combination of a research-grade DMA (dynamic mechanical analyzer) and an FTIR (Fourier transform infrared) spectrometer is demonstrated in simultaneous mechanical analysis and dynamic IR spectral measurement. In such a study, molecular-level responses to the deformation can be observed in the dynamic IR spectra and used to better understand the macroscopic viscoelastic behavior of the polymer sample characterized by monitoring the stress and strain. The measurements are performed on polymer films, with the DMA in the tensile geometry and IR measurement in the transmission mode. The DMA−FTIR technique is demonstrated in the creep−recovery study of an industrially important elastomer, Estane 5703. Differential orientation of various segments of the macromolecule during the creep and recovery process is observed. In a novel molecular-level application, Burger's model, a viscoelastic model that is often used to explain the bulk properties of materials, is applied to the analysis of the orientation of individual infrared dipoles. By replacing strain with orientation functions, contributions from separate molecular moieties to the macroscopic elasticity and viscosity are differentiated. Permanent damage observed after a large displacement is attributed to the irreversible alteration of the microscopic network structure of the elastomer and is discussed in light of IR spectral changes during the creep−recovery process.

Introduction

Studies of structure−property relationships have always been and continue to be an important aspect of research related to polymers.[1] Knowledge of the effect of chemical structure and physical state on mechanical properties serves as invaluable guidance for the development of new polymers with distinctive combinations of properties such as strength, stiffness, elasticity, and damping. Studies of structure−property relationships rely heavily on techniques that allow not only measurement of physical properties of the materials on the macroscopic scale but also probing of the microscopic structures on the molecular and morphological scale. The development and application of these techniques are important components of polymer characterization.

The most practical way of determining macroscopic mechanical properties is achieved through dynamic mechanical analysis (DMA),[2,3] in which a sample is subjected to a specific mechanical perturbation with the resulting strain−stress response being monitored. The stress and strain as a function of time are then used to calculate a variety of material viscoelastic parameters that can be further used to determine the processability and end-use performance of materials. On the other hand, FTIR spectroscopy is one of the primary techniques for polymer characterization on the molecular scale.[4−6] In the IR spectrum, each functional group of a polymer generally exhibits distinctive absorption bands, and the band energies, intensities, and shapes contain information about polymer crystallinity, molecular orientation, and conformational regularity.

In recent years, vibrational spectroscopists have been particularly interested in combining DMA with vibrational spectroscopy in an effort to correlate the macroscopic properties of polymers with their molecular origins.[5,6] IR and Raman spectroscopic investigations of polymers under mechanical load, during elongation,[7−10] and subjected to sinusoidal reversible perturbation have been reported.[11−13] Because the DMA measurements often involve stressing, deforming, heating, or cooling of the sample under a particular time function specified by the user, it is desirable for vibrational spectra to be collected as a function of time as well. This approach allows for the correlation of the real time spectral information with the stress−strain responses as well as other derived parameters of the material.

DMA−FTIR studies generally fall into two categories. In the first experimental approach, large-amplitude (irreversible), long-time linear deformation is applied on the sample by use of the DMA. At the same time, continuous- or rapid-scan FTIR time-resolved spectral measurements are performed so that each spectrum recorded is effectively instantaneous on the time scale of the experiment.[5,14] Creep−recovery and stress−relaxation are the two most popular DMA modes used in these studies. Simultaneous IR data with time resolution as fast as 10 ms and as long as days or weeks can be collected in such experiments with current continuous-scan FTIR technology.

The second approach utilizes the oscillatory deformation mode, in which sinusoidal stress−strain perturbation is applied on the sample. Storage modulus, loss modulus, and tan δ are obtained by analyzing the relative magnitude and phase of the stress and strain signals. The sinusoidal amplitude is small, within the linear deformation range of the material, and therefore both the mechanical and the spectral responses are

[†] Duke University.
[‡] Los Alamos National Laboratory.
[§] TA Instruments, Inc.
* Corresponding author: Email rap@chem.duke.edu; phone (919)-660-1539; Fax (919)-660-1605.

10.1021/ma001783b CCC: $20.00
Published on Web 08/24/2001

repeatable from cycle to cycle. Current state-of-the-art, *step-scan* FTIR instruments can provide phase-resolved dynamic in-phase and quadrature spectra (spectral responses in-phase with and 90° out-of-phase with the strain perturbation) which are related directly to storage modulus and loss modulus, respectively.[15−20]

In this work, we demonstrate the use of a combination of a commercially available research-grade DMA and a FTIR spectrometer in simultaneous mechanical analysis and dynamic IR spectral measurement of a polymer under large-amplitude creep deformation. By careful analysis of the time-resolved IR data, dynamic molecular orientational motions in response to the deformation can be studied and used to explain the macroscopic viscoelastic behavior of the polymer sample studied.

The DMA−FTIR technique is demonstrated in the creep−recovery studies of Estane 5703. Estane is the name given to a family of poly(ester urethane) segmented copolymers. In these materials, the polyurethane segments associate with one another to form hard domains which act as pseudo-cross-links between the polyester soft domains. In the infrared spectrum of this polymer the distinctive primary bands arise from vibrations of functional groups such as C−O−C groups of both the urethane and ester, the phenyl rings of the urethane, the N−H and C−N groups of urethane, the C═O groups of both domains, and the CH_2 groups of both domains.

Differences in the orientation responses of various parts of the macromolecule during the creep−recovery process are observed and quantitatively compared. In this comparison, a novel analysis of the dynamic IR dichroic data in terms of the Burger model is used. This model, composed of a combination of springs and dashpots and often used to describe the macroscopic viscoelastic behavior of materials, is applied here to the analysis of the orientation functions of individual functional groups of Estane. This approach leads to the conclusion that the permanent damage of the material observed after a large displacement is due to the irreversible destruction of the microscopic network structure of the elastomer. These effects are revealed in IR dichroic spectral changes during creep and recovery and in the pattern of "microscopic" Burger parameters derived from the data.

Experimental Section

Instrumentation and Sample Preparation. A TA Instruments research-grade dynamic mechanical analyzer (DMA2980) has been optically interfaced with a Bruker Optics research-grade FTIR spectrometer (IFS66/DSP). The DMA is operated in the tension mode. Films of Estane [poly(butylene adipate)-poly(4,4′diphenylmethane diisocyanate-1,4-butanediol] were solvent cast from pellets using methyl ethyl ketone. The 10 μm thick free-standing films of Estane were cast on Teflon sheets followed by vacuum-drying. Samples were removed from the Teflon and mounted in the standard tensile jaws of the DMA. An accessory for interfacing the DMA to the FTIR has been built that can be easily attached to the spectrometer and aligned to achieve optimal performance. Infrared radiation from an external port of the FTIR is directed and focused onto the sample, and the transmitted light is then refocused on a liquid nitrogen-cooled mercury−cadmium−telluride (MCT) detector outside the spectrometer bench. A flexible polyethylene enclosure is used to extend the dry air purge of the FTIR spectrometer to include the external beam path.

To monitor the orientation events associated with the approximately uniaxial strain, a wire grid IR polarizer is placed just in front of the sample. The polarizer can be manually switched between parallel and perpendicular to the stretching direction. Polarized absorption data in the two directions are collected in separate runs on different samples. The polarized results measured from different experiments are found to be extremely reproducible from sample to sample and run to run. The data were measured in the creep−recovery mode at room temperature (about 25 °C). For each run, a fresh sample was cut and mounted. The experimental profile started with a 2 min equilibration (0.05 N loaded on the freshly prepared film). Then, the load on the film was instantaneously (in less than 0.3 s) increased to 0.3 N where it was maintained for 30 min, after which the tension on the polymer was released back to 0.05 N for another 30 min. The use of the 0.05 N load on the polymer during the initial and final stages of the creep experiment serves to prevent the polymer film from buckling.

The FTIR spectrometer was triggered by the DMA, so that data collection of the DMA and spectral measurement of the time-resolved, polarized IR proceeded in parallel. The FTIR instrument operated in the standard, constant-velocity, or rapid-scan transmission mode, with a spectral resolution of 4 cm^{-1}. With a scan repetition rate of 10 Hz, the FTIR bench demonstrated an effective maximum time resolution of 0.1 s, with no coaddition of scans. In this manner, for each run, a stack of spectra was measured, each of which corresponds to the polarized absorption of the film at a specific time during the creep−recovery process.

The time interval of the collection and averaging of the time-resolved IR spectra was adjusted to the rate of response. At times when a rapid sample or spectral change was expected, fewer coadditions were used to ensure spectra of higher time resolution. During periods when a slow sample or spectral change was expected, more coadditions were used, yielding spectra with lower, but sufficient, time resolution. Even at the lower coadditions, the SNR was more than adequate for the analysis.

For the results reported here, four measurements (each on a different sample) were preformed, with two using parallel polarization and two in the perpendicular polarization. All the time-resolved single beam spectra were converted to time-resolved absorption spectra by referencing to their corresponding blank single-beam spectra. Then, the IR data at the same polarization were averaged to afford one set of time-resolved IR absorption spectra for each polarization, which was then used for further analysis. Such a measurement method relies on the high reproducibility of the creep experiments, especially the reproducibility of sample cutting and mounting. For the measurements described here, films of exactly the same size were cut and then mounted on the DMA in a controlled and reproducible fashion. The film dimensions were 60 mm long, 9.0 mm wide, and 0.01 mm thick.

Theory

Burger's model is a theoretical approach that utilizes a combination of dashpots and springs to model macroscopic visoelastic behavior of materials.[21,22] In this and similar rheological models, pure elastic behavior is represented by a Hookean spring, while pure viscous behavior is represented by a Newtonian dashpot.

When all the inertial effects are neglected, the stress−strain responses of a spring obey Hook's law; i.e., the magnitude of the strain is directly proportional to the stress

$$\sigma_e = E\gamma_e \tag{1}$$

where E is the spring constant and represents the elasticity. On the other hand, the behavior of an ideal viscous fluid, represented by the dashpot, follows Newtonian law; i.e., the strain *rate* is proportional to the stress,

$$\sigma_\eta = \eta \, \mathrm{d}\gamma_\eta/\mathrm{d}t \tag{2}$$

where η represents the viscosity, and σ_η and $\mathrm{d}\gamma_\eta/\mathrm{d}t$ are the stress and the strain rate, respectively.

Elasticity describes a material's ability to store energy and is independent of time. The rheological response of a purely elastic material is instantaneous. On the other hand, viscosity is defined as a material's resistance to flow. Because of internal friction, viscous materials respond to an external perturbation slowly; i.e., the rheological responses of viscous materials are time-dependent. Thus, under the condition of a creep experiment, when a load σ_e is instantaneously applied on a spring, the spring responds instantaneously with a strain γ_e, equal to σ_e/E. When the load is suddenly removed, the spring immediately recovers to its original length. For a viscous fluid (dashpot), a constant strain rate is expected when a constant load is applied. The strain as a function of time can be obtained by integrating the strain rate.

$$\gamma_\eta = \sigma_\eta t/\eta \tag{3}$$

The plot of γ_η as a function of time is a straight line, the slope of which is a constant proportional to the load. When the load is suddenly removed, strain rate becomes zero and the fluid remains in the deformed state.

Viscoelastic materials can be modeled by a combination of Hookean springs and Newtonian dashpots. The simplest of these, the Voigt (Kelvin) model, consists of a spring and a dashpot in parallel to each other. The constraint on the model is that the strain must be the same in both elements, and the stress must be the sum of the stresses from the two elements.

$$\gamma_K = \gamma_e = \gamma_\eta \tag{4}$$

$$\sigma_K = \sigma_e + \sigma_\eta = E\gamma_e + \eta \, \mathrm{d}\gamma_\eta/\mathrm{d}t \tag{5}$$

Integration of eq 5 provides the time function of strain.

$$\gamma_K = \sigma/E[1 - \exp(-E\, t/\eta)] \tag{6}$$

The indices *e* and η are omitted because the strain is the same in both elements. The change of the strain in such a case follows an exponential decay.

Materials exhibiting a more complex rheological behavior can often be characterized in terms of a Burger model. Figure 1 shows the typical creep curve of a Burger model. The Burger model features a spring, a Voigt element, and a dashpot, in series. With this model, the total deformation must be the sum of the deformation of each element.

$$\gamma = \gamma_e + \gamma_K + \gamma_\eta \tag{7}$$

Adding eqs 1, 3, and 6 gives

$$\gamma = \sigma/E + \sigma/E_K[1 - \exp(-E_K\, t/\eta_K)] + \sigma t/\eta \tag{8}$$

The advantage of such a four-parameter model is that, just as the model is comprised of three basic elements, so the response curve can also be divided into three distinct regions. The first region is the Hookean region, which is the instantaneous extension at the beginning of the creep profile. For a Hookean spring, as soon as the load σ is applied, the spring deforms to $\gamma_e = \sigma/E$.

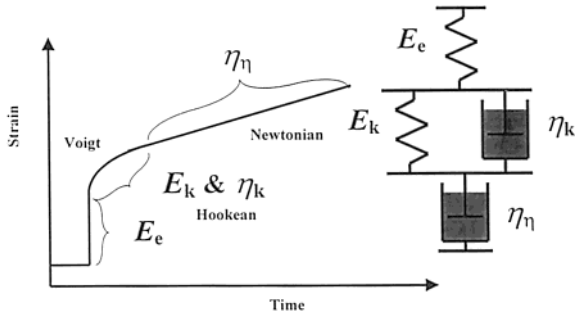

Figure 1. Quantitative analysis of the creep curve of the Burger model of viscoelasticity.

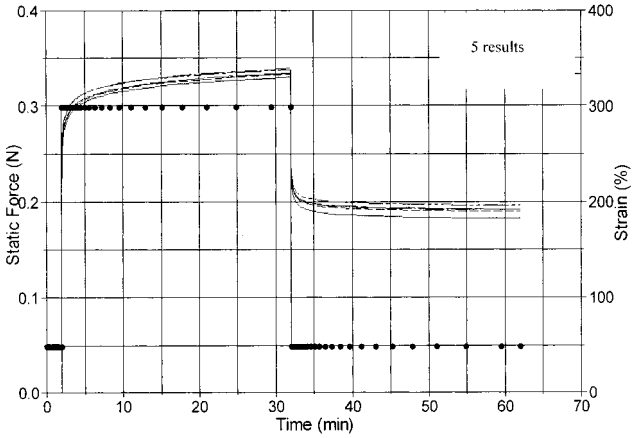

Figure 2. DMA creep−recovery data obtained from five separate experiments of five different Estane films.

Table 1. Viscoelasticity Parameters of Estane Obtained from Burger Modeling of the Creep Data

E_e (10^6 Pa)	E_k (10^6 Pa)	η_k (10^8 Pa s)	η_η (10^{10} Pa s)	recovery (%)
1.09	4.71	5.06	2.98	44.6

After the material is loaded, the same load is also applied onto the Voigt element and the Newtonian element. Unlike the Hookean element, which responds instantaneously, their deformation is time-dependent and therefore contributes to the second and the third regions (the Voigt and the Newtonian regions). This behavior manifests itself as an exponential decay on top of a slope. As it approaches the third region, the Voigt element slowly reaches its equilibrium state and its maximum deformation, and the material deformation is predominantly creep due to the dashpot. Ideally, as long as the dashpot is loaded, such a creep will not stop and will continue at a constant rate. Hence, the third region resembles a straight line, the slope of which is determined by η.

Results

The DMA data from five sequential creep−recovery experiments are shown in Figure 2. During each of these experiments either the parallel or perpendicular polarized IR absorption was measured simultaneously with the DMA data. The reproducibility of the DMA data from run to run (±3%) supports the validity of using the IR data from sequential runs to calculate the dichroic difference spectra (see below).

A Burger model has been applied to the average of the creep−recovery data shown in Figure 2. The four parameters of the model obtained are listed in Table 1.

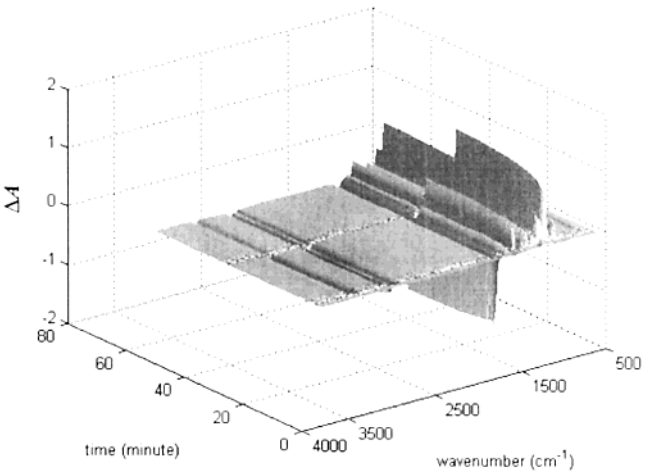

Figure 3. Dichroic difference spectra of Estane during the creep and recovery, corrected for thinning.

The percentage of the strain recovery of the polymer at the end of the measurement is also calculated and listed in Table 1.

The IR data ($A_{\parallel}(\sigma,t)$ and $A_{\perp}(\sigma,t)$) are corrected for the thinning effect of the film, by reference to the structural absorption $A_0(\sigma,t)$,[5] where

$$A_0 = \frac{A_{\parallel} + 2A_{\perp}}{3} \tag{9}$$

By assuming that A_0 for uniaxial stretching is independent of the chain orientation of the polymer but dependent on the film thickness, the change of the structural absorption spectrum due to thickness variations of the polymer film during the creep and recovery process $A_0(\sigma,t)$ can be calculated.[5] This calculation allows the quantification of thickness change of the sample, which is then used to compensate for the thinning effect in the dichroic difference calculation. In this way, corrected dichroic difference spectra ($\Delta A(\sigma,t) = A_{\parallel}(\sigma,t) - A_{\perp}(\sigma,t)$), corresponding to a sample of effectively constant thickness, were calculated (Figure 3). (In fact, the stretching is only approximately uniaxial owing to the width of the sample necessary to intercept the IR beam diameter. However, this is not a problem since the analysis and conclusions do not presume strictly uniaxial strain.)

To quantify these dichroic difference spectra, the data are first converted into orientation functions for the vibrational bands corresponding to the various functional groups.[7,23,24] If the usual simplifying assumption is made that ψ, the angle between the polymer chain axis and each of the vibrational dipoles, is equal to either 0 or 90°, the equations for calculating the orientation function f simplify to the following forms:

$$f_{\parallel} = \frac{R-1}{R+2} \quad \text{for } \psi = 0° \tag{10}$$

$$f_{\perp} = -2\frac{R-1}{R+2} \quad \text{for } \psi = 90° \tag{11}$$

In these equations, R is the dichroic ratio of a given absorption band. Results of such calculations for two selected of bands are shown in Figure 4.

The orientation function of each band was calculated from the integrated absorption within a specific bandwidth. The carbonyl region of this copolymer is highly

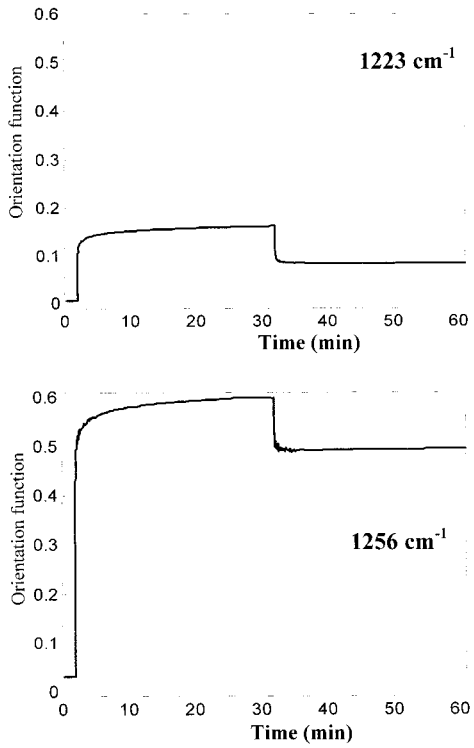

Figure 4. Change of orientation function of selected functional groups of Estane during the creep−recovery experiment.

overlapping, originating from both the carbonyl group of the polyester and the amide I group of the polyurethane. Each of these components is further split due to various forms of inter- and intramolecular interactions, especially hydrogen bonding. In this paper, the carbonyl region is treated as a single band; the results, therefore, gauge the effect of the commbination of the ester and urethane carbonyl components.

The orientation functions for 14 selected absorption bands calculated as a function of time during the creep−recovery experiment were then individually least-squares fit to the Burger model equation. The results of applying the Burger model to the creep−recovery IR orientation functions of each of the functional group frequencies are shown in Table 2. In each column of Table 2 the five largest values are selected with their cells rendered in gray, while the five smallest values are selected with the text highlighted in a darker gray.

Discussion

Since polymers are viscoelastic materials that have combined mechanical properties of elastic solids and viscous fluids, they respond to an external force in a manner intermediate between the behavior of an elastic solid and a viscous fluid.[21,22] Burger's model provides a mechanism to gain insight into this behavior. The DMA creep−recovery curve for Estane resembles the response predicted by Burger's model, suggesting that the macroscopic viscoelasticity of the polymer may be understood in terms of this model. The large time-independent, virtually instantaneous strain upon the impulsive increase of the stress indicates elastomeric behavior with a weak Hookean constant. The weaker the Hookean constant, the larger the initial fast displacement. After the weak Hookean spring reaches its maximum displacement, the polymer slowly shifts through the curvature of the Voigt region to the Newtonian region. The creep response is time-dependent and indicates the

Table 2. Parameters Obtained from Burger Modeling of the Creep Data for Infrared Bands

frequency (cm^{-1})	domain origin	E_e (10^7 Pa)	E_k (10^7 Pa)	η_k (10^9 Pa s)	η_η (10^{11} Pa s)	recovery (%)
3342	hard	1.61	6.90	5.45	2.36	32.9
3125	hard and soft	1.56	8.53	4.85	6.83	27.2
1732	hard and soft	1.36	7.35	1.57	3.48	26.0
1597	hard	2.01	6.62	2.72	3.29	55.3
1533	hard	1.77	5.89	7.47	2.65	48.9
1464	soft	1.48	6.24	4.04	3.13	39.8
1362	soft	0.86	4.05	6.23	2.17	37.7
1311	hard	1.60	7.49	5.87	2.71	42.6
1256	soft	0.59	2.72	6.62	1.64	17.5
1223	hard	2.42	8.30	7.36	3.43	48.0
1174	soft	1.08	3.67	6.21	1.74	28.6
1143	soft	1.50	1.58	7.39	0.60	35.2
1074	hard and soft	1.56	4.87	8.51	2.14	45.1
1019	hard	1.34	5.47	6.87	2.05	40.2
average		1.43	5.69	5.80	2.73	37.5

yielding of the polymer to the stress by reorganization of its internal microscopic structure. The creep rate of Estane is indicative of the stability of its elastomer structure. When, after 30 min of constant stress, the stress is suddenly reduced back to 0.05 N, the polymer is able to recover from almost half of its maximum elongation. This is consistent with moderate elastomeric stability.

Figure 2 also shows the high reproducibility of the DMA data measured from different samples. This high reproducibility validates the use of the polarized data from two separate measurements of two different samples for calculating the dichroic difference and dichroic ratio.

Normally, three types of spectral changes appear in the time-resolved infrared data. These changes include (1) a decrease of the absorption intensity due to the thinning of the stretched polymer film, (2) a change in absorption intensity due to the strain-induced orientation of the molecular chains and functional groups, and (3) an infrared absorption band frequency shift due to the distortion of the torsion angles, bond angles, or bond lengths or to strain-induced crystallization.

Although the thinning provides insight into the deformation of the material, in this experiment, the interest is in the orientations of the individual functional groups of the macromolecule and the time profiles of their responses in comparison with the macroscopic creep curve. The thinning effect-corrected, dichroic difference data in Figure 3 demonstrate that the backbone vibrational modes (transition dipole moments parallel to the chain direction) orient toward the stretching direction with positive dichroic difference bands. In contrast, the vibrational modes of the side groups (e.g., C═O stretching, N−H stretching, C−H stretching) orient toward the perpendicular direction. The change in the dichroic band after the impulse stress increase and the impulse stress release follows a specific dynamic curve for each band. However, quantification and detailed differentiation of the responses of different bands are not easily accomplished from the ΔA data. Burger's model using infrared bands aids in this analysis.

The calculation of orientation functions is a method for normalizing the dichroic data for different absorption bands. The orientation function of each band is independent of the dipole moment strength of the corresponding vibrational mode. It is also independent of the thinning effect since it is based on the *ratio* of the dichroic data rather than their difference. Orientation functions are often used to compare different static states of a material. In the current data, the orientation functions of the characteristic bands of Estane are examined dynamically during the entire course of the creep−recovery process. If all the segments of the macromolecule orient uniformly in response to the stress, the orientation functions calculated from IR absorptions of different functional groups should follow exactly the same dynamic curve. However, as indicated by the sample curves shown in Figure 4, different parts of the macromolecule have distinctly different dynamic responses in the creep−recovery process.

Each of the orientation functions demonstrates a unique temporal magnitude and shape. To quantitatively compare the differences between the orientation functions calculated from different vibrational bands, the data from each band were fitted to a Burger model. In the fitting process the time function of strain (γ) is replaced by the time function of the orientation function of the bands, which is designated the "strain orientation function". Similar to the conventional strain, the strain orientation function is dimensionless. As in the analysis of the DMA data, Burger modeling of each IR band can provide four basic parameters. By comparing each of the four parameters from different vibrational bands, insights can be gained concerning the degree to which orientation of each functional group (and the segmental component of the domain) contributes to the elasticity and viscosity of the material.

In Tables 1 and 2, the values of E_e and E_k correspond to the modulus in the Hookean and Voigt regions of the creep response, respectively. The general magnitude of these parameters is an indicator of strength, with larger values corresponding to smaller strain orientations reached for a given amount of stress. In Table 2 the Hookean E_e values differentiate the bands from the hard and soft segments, with the hard segments generally possessing higher modulus values ($E_e(\text{soft})/E_e(\text{hard})_{avg} = 0.618$). This observation indicates that, during the initial stage of the impulse time-independent elastic deformation, the soft domains orient more, contributing more to the macroscopic deformation, while the hard domains orient less, contributing more to the elasticity or Young's modulus (initial strength). These data agree with previous results from the static stretching of Estane films.[23] The soft domains are above their T_g and thus have more mobility than the hard domains. The hard domains cannot achieve a fast orientation response to the sudden increase of stress. While the relative magnitudes are slightly different between the different bands, the trend observed for E_k (Voigt region) is similar to that observed for E_e ($E_k(\text{soft})/E_k(\text{hard})_{avg} = 0.539$).

The analysis of the parameter η_η provides insights into the slow structural rearrangement of the elastomer morphology after it is already stressed and deformed. Elastomers have two major structural characteristics: (1) a major portion of the polymer is above its T_g, and (2) the polymer has a stable network structure (physical or chemical). The polymer then has mobility to deform, and even after it has been strained several times its original length, the network structure is not significantly changed. As a result, upon the release of the stress, the polymer is able to recover to nearly its original length. While the Hookean (initial) region provides insights into the mobility of the morphological structure, the Newtonian region provides insights into the stability of the network structure. The slow change in this region is characteristic of the motion of a highly viscous material that undergoes slow but steady irreversible changes.

The parameter η_η corresponds to viscosity in the dashpot element of the Burger model. Bands with a large η_η are associated with a slow change and, as seen in Table 2, predominately correspond to the hard segments (η_η(soft)/η_η(hard)$_{avg}$ = 0.639). Bands with small η_η tend to be associated with the soft domains. The hard domains, therefore, play a vital role in the polymer as the predominant network structure. The low mobility of the hard domains preserves the memory of the network structure.

The data indicate that the network structure changes slowly and irreversibly in the Newtonian region. The percentage lack of recovery is indicative of the degree of irreversible damage of the network structure. The carbonyl band (1732 cm^{-1}; hard and soft segment components) is among those that do not completely recover even though it is the least orientated band in the Hookean region and the slowest band to change in the Newtonian region. Interestingly, the lowest recovery occurs for the 1256 cm^{-1} band, the ν(C−O−C) vibration in the soft segment backbone. The frequency of this band was previously observed to shift significantly upon stretching but to shift back upon relaxation.[24] The associated damage caused appears to be irreversible and most likely involves some changes in hydrogen-bonding interactions. These functional groups are known to be involved in hydrogen bonding.

In Table 2, the bands with the largest recovery are from hard segment bands at 1597, 1533, 1311, 1223, and 1074 cm^{-1} (average 46.9% recovery). These bands have significant contributions to their normal modes from backbone polymer stretches including ν(C═C) of the phenyl ring, ν(C−N) of the polyurethane, and ν(C−O−C) of the polyurethane. Soft segment bands, with their lower E_e values and higher chain mobility and distortion, undergo larger changes. These soft segment functional groups are not able to recover to the same degree as the hard segment groups because of the large distortion (average 31.8% recovery). It is interesting to note that this analysis in terms of the Burger model leads to conclusions in terms of relative recovery of hard and soft segments that are at variance with some earlier studies.[7,25] However, the extent of recovery for the different segments is dependent upon the percentages of hard and soft segments and the chain length of the segments. In the current study, the polymer is relatively soft, with 75% soft and 25% hard domains. The long soft segment chains cause greater entanglements and interactions which lead to less recovery in this polymer.

The last row of Table 2 lists the value of the parameter in each column, averaged over all the IR frequencies in the table. It is interesting to note that the ratios of the averages of the four microscopic (IR) parameters (1:3.99:4.07:1.92) are similar to the corresponding ratios for the macroscopic parameters (1:4.32:4.64:2.74) and that the average percent recovery in the orientation functions is ca. 40% compared to 45% for the strain. These bands represent the major contributors to the dynamic spectrum. The rough agreement between the ratio of the macroscopic parameters and the ratio of the averaged microscopic parameters suggests that the simplifying assumptions used in calculating the strain orientation functions are valid for a relevant interpretation of the IR data. (The approximate 10-fold difference in the values of the two sets of parameters is simply a reflection of the extent of the relative strain compared to the fixed range of the value of the orientation function (−0.5 to 1.0). The units of the two sets are the same owing to the unitless quality of both the relative strain and the orientation function.)

Conclusions

This is the first report of the integration of a research-grade DMA and FTIR for simultaneous, *quantitative* macroscopic and microscopic dynamic characterization of polymer materials. This integrated approach has been demonstrated in the creep−recovery characterization of the copolymer Estane 5703 at ambient temperature. Orientations of various parts of the macromolecule during the creep−recovery process have been inferred from the IR data, and orientation behaviors of different parts of the molecule have been differentiated. Burger's model has been used for the quantitative analysis of both the macroscopic (stress−strain) rheology and microscopic rheology, as represented by the time dependency of the IR orientation functions of various functional groups. In this analysis of the "strain orientation function", modulus values were obtained for individual IR bands; these values were significantly different for the hard vs soft segment bands, consistent with earlier observations of relative orientations upon stretching. The permanent damage of the material after a large displacement creep is attributed to the irreversible destruction of the microscopic structure (likely hydrogen bonding) of the elastomer. The hard segments show a higher percentage of recovery than the soft, indicating that the hard segment functional groups are less susceptible to the damage that can occur with the higher mobility, characteristic of the soft segment functional groups.

The flexibility and capability of the DMA allow the application of various modes of dynamic deformation. The available deformation modes include creep−recovery, strain relaxation, and sinusoidal deformation at various frequencies, as well as others, which are the scientific and industrial standards for viscoelasticity characterization of polymers. The experimental approach described here, combining DMA with simultaneous molecular characterization by dynamic FTIR, and analysis of both macroscopic and microscopic data sets in terms of a common model significantly extends the scope of polymer optorheological investigation.

Acknowledgment. The authors gratefully acknowledge the assistance of The Lord Foundation of North Carolina, Bruker Optics, TA Instruments, and Duke

University for support of this work. Work at Los Alamos National Laboratory was performed under the auspices of the U.S. Department of Energy with support from the Laboratory Directed Research and Development Program and the Technology Partnership Program at Los Alamos.

References and Notes

(1) Seymour, R. B.; Carraher, C. E., Jr. *Structure−Property Relationship in Polymers*; Plenum Press: New York, 1984.
(2) Mark, J. E.; Eisenberg, A.; Graessley, W. W.; Mandelkern, L.; Koenig, J. L. *Physical Properties of Polymers*; American Chemical Society: Washington, DC, 1984.
(3) Haines, P. J. *Thermal Methods of Analysis*; Plackie Academic and Professional: Glasgow, 1995.
(4) Griffiths, P. R.; de Haseth, J. A. *Fourier Transform Infrared Spectrometry*; John Wiley and Sons: New York, 1986.
(5) Siesler, H. W.; Holland-Moritz, K. *Infrared and Raman Spectroscopy of Polymers*; Marcel Dekker: New York, 1980.
(6) Fawcett, A. H. *Polymer Spectroscopy*; John Wiley & Sons Ltd.: Chichester, 1996.
(7) Siesler, H. W. *Polym. Bull.* **1983**, *9*, 382−389.
(8) Kalkar, A. K.; Pfeifer, F.; Siesler, H. W. *Macromol. Chem. Phys.* **1998**, *199*, 667−675.
(9) Molis, S. E.; MacKnight, W. J.; Hsu, S. L. *Appl. Spectrosc.* **1984**, *38*, 529−537.
(10) Heymans, N. *Polymer* **1987**, *28*, 2009−2017.
(11) Noda, I.; Dowrey, A. E.; Marcott, C. *Appl. Spectrosc.* **1988**, *42*, 203−216.
(12) Noda, I.; Dowrey, A. E.; Marcott, C. *J. Polym. Sci., Polym. Lett.* **1983**, *21*, 99−103.
(13) Chase, B.; Ikeda, R. *Appl. Spectrosc.* **1993**, *47*, 1350−1353.
(14) Pezolet, M.; Buffeteau, T. Study of Polymer Orientation and Relaxation by Polarization Modulation and 2D-FTIR Spectroscopy. Presented at AIRS III, Vienna, Austria, July 1998.
(15) Marcott, C.; Dowrey, E. A.; Noda, I. *Appl. Spectrosc.* **1993**, *47*, 1324−1328.
(16) Palmer, R. A.; Manning, C. J.; Chao, J. L.; Noda, I.; Dowrey, A. E.; Marcott, C. *Appl. Spectrosc.* **1991**, *45*, 12−17.
(17) Gregoriou, V. G.; Noda, I.; Dowrey, A. E.; Marcott, C.; Chao, J. L.; Palmer, R. A. *J. Polym. Sci., Part B: Polym. Phys.* **1993**, *31*, 1769−1777.
(18) Palmer, R. A.; Gregoriou, V. G.; Fuji, A.; Jiang, E. Y.; Plunkett, S. E.; Connors, L. M.; Boccara, S.; Chao, J. L. In *Multidimensional Spectroscopy of Polymers*; ACS Symposium Series 598; Urban, M. W., Provder, T., Eds.; American Chemical Society: Washington, DC, 1995; pp 99−116.
(19) Budevska, B. O.; Manning, C. J.; Griffiths, P. R.; Roginski, R. T. *Appl. Spectrosc.* **1993**, *47*, 1843−1851.
(20) Ingemey, R. A.; Strohe, G.; Veeman, W. S. *Appl. Spectrosc.* **1996**, *50*, 1360−1365.
(21) Elias, H. *Macromolecules*, 2nd ed.; Plenum Press: New York, 1984.
(22) Aklonis, J. J.; MacKnight, W. J. *Introduction to Polymer Viscoelasticity*; John Wiley & Sons: New York, 1983.
(23) Wang, H.; Graff, D. K.; Schoonover, J. R.; Palmer, R. A. *Appl. Spectrosc.* **1999**, *53*, 687−696.
(24) Graff, D. K.; Wang, H.; Palmer, R. A.; Schoonover, J. R. *Macromolecules* **1999**, *32*, 7147−7155.
(25) Seymour, R. W.; Cooper, S. L. *Rubber Chem. Technol.* **1974**, *47*, 19−31.

MA001783B